

Density of State Effects in Ag $L_3M_{4,5}M_{4,5}$ Threshold Auger Spectra

W. Drube, R. Treusch, and G. Materlik

*Hamburger Synchrotronstrahlungslabor HASYLAB am Deutschen Elektronen-Synchrotron DESY,
Notkestrasse 85, D-22603 Hamburg, Germany*

(Received 15 July 1994)

The energy distribution of $L_3M_{4,5}M_{4,5}$ Auger electrons emitted from solid Ag is studied as a function of the exciting photon energy in the L_3 threshold region. The 1G_4 Auger line not only exhibits a Raman-type energy dispersion and a reduced core hole lifetime broadening, but its line shape is also markedly modulated. For subthreshold excitation, additional structure appears within the highly asymmetric emission profile. This is interpreted as being due to the local density of empty d states probed in the intermediate dipole transitions. A simple numerical model qualitatively reproduces the gross features of the measured electron distribution.

PACS numbers: 32.70.Jz, 32.80.Hd, 79.60.Bm

The creation of an atomic inner shell vacancy by photons induces a complex dynamical multielectron response of the electronic system. Auger electrons emitted in the deexcitation process can be used as a sensitive probe to study electron-electron correlations in atoms, molecules, and solids [1]. It has long been known that the conventional two-step model of the Auger process fails if the excited hole state decays before its relaxation is complete [2]. In particular, for near threshold excitation creation and decay of an inner shell hole are not distinct processes but have to be viewed as a single-step event [3,4].

An interesting situation arises if the energy $\hbar\omega$ of the exciting radiation is so well defined that the interaction time $\Delta\omega^{-1}$ is comparable to or even longer than the lifetime \hbar/Γ of the resonant state. Then the emission, i.e., Auger electrons and fluorescence radiation, is an integral part of the excitation process itself and strongly depends on the excitation energy. The dynamics of threshold excitation can thus be probed experimentally if the spectrum of emitted particles is measured to be highly energy resolved, i.e., on the scale of the lifetime broadening Γ . The progress in experimental techniques and the availability of high-flux synchrotron radiation beam lines have only recently stimulated rapidly growing research in this field, although still only a few studies exist for the radiationless process [5–15].

It was discovered [5,6] that the Xe $L_3M_4M_5(^1G_4)$ Auger spectrum excited in the vicinity of the L_3 edge, exhibits a behavior characteristic of a resonant Raman transition (Auger resonant Raman effect): $5d$ and $6d$ spectator satellite lines were observed which disperse linearly with the exciting photon energy and are resonantly enhanced at the $2p_{3/2} \rightarrow nd$ threshold. Also, their observed linewidth is not limited by the inner-shell hole lifetime but dependent on the exciting photon energy distribution. An analogous behavior has very recently been reported for atomic and molecular resonant Auger processes involving comparably long-lived shallow core levels [10,12].

In solids, a similar effect is found for ionic materials [9], SiO_2 [7,13], Ge [8], and InP [14] and also ascribed to discrete excitations, in the sense of excitonic states, which result in a spectator-type transition. Even for open shell $4d$ metals, Rh and Pd, strongly dispersing resonance lines were observed in $L_3M_{4,5}M_{4,5}$ spectra [11] and attributed to localized $2p_{3/2} \rightarrow 4d$ excitations.

The observed behavior of the resonance lines is in general agreement with the predictions of time-independent resonant scattering theory [3,4,6] for the threshold Auger process in free atoms. There they correspond to excitations of the inner shell electron into excited bound (spectator) states. The normal Auger line, however, derives from transitions into the continuum. For subthreshold excitation, also referred to as the resonant Raman regime, a continuous electron distribution is predicted, highly asymmetric, which evolves into the characteristic Auger line above threshold [4].

In this study we are focusing on this gradual transition. Moreover, it is interesting to elucidate the influence of the solid state environment on the threshold Auger process. We investigated the $L_3M_{4,5}M_{4,5}$ Auger transition of Ag, for which a broad conduction band is formed with a low content of d states. Pronounced modulations of the 1G_4 line are observed as a function of the photon energy. Below threshold a highly asymmetric profile is measured which is characteristic of the continuous radiationless resonant Raman scattering [4]. In addition, an extra structure appears which can be related to the partial density of empty d states probed by the excited photoelectron in the $2p_{3/2} \rightarrow 4d$ transition.

The experiment was performed at the high-flux wiggler beam line BW2 at HASYLAB [16], Hamburg, Germany, using synchrotron radiation from the DORIS III storage ring. Briefly, intense continuous radiation from a 56-pole x-ray wiggler is reflected by a plane premirror onto a (+/-) Si(111) double crystal monochromator. The monochromatic beam is focused by a toroidal mirror onto a high-purity (99.99%) Ag foil, cleaned by repeated Ar

sputtering and annealing cycles. The kinetic energy of the emitted electrons is determined using a hemispherical electron analyzer set to an energy resolution of 0.5 eV FWHM. The photon flux in the focal spot ($\approx 1 \times 1 \text{ mm}^2$ FWHM) on the sample amounts to $1 \times 10^{12} \text{ sec}^{-1}$ with a measured spectral width of 0.7 eV FWHM at 3350 eV.

In the following, we reference the photon energy relative to the Ag L_3 excitation threshold taken as the inflection point of the L_3 absorption edge, which is measured by recording the total electron yield from the sample. The edge position was carefully determined and frequently checked during the experiment to yield an accuracy of $\pm 0.1 \text{ eV}$ for the relative photon energy. The absolute threshold energy is near 3351 eV corresponding to the tabulated $2p_{3/2}$ binding energy [17].

The Ag $L_3M_{4,5}M_{4,5}$ Auger spectrum (Fig. 1) reveals distinct emission lines which can be associated with the multiplet components of the $M_{4,5}M_{4,5}$ two-hole final state if compared to calculated values [18,19]. The prominent peak at $2576.8 \pm 1 \text{ eV}$ corresponds to the 1G_4 final state for which the highest transition rate is calculated. The excitation energy is 1.0 eV above threshold and the emission exhibits resonant behavior: The Auger lines are considerably narrower than compared to off-resonance excitation [18–20], where their width is determined by the combined intermediate and final state lifetimes. Here, the intermediate state lifetime (2.05 eV, see below) does not yet fully contribute to the measured width resulting in an asymmetric line shape with a smaller apparent FWHM [4]. This is most notably seen for the 1G_4 peak. The careful analysis of our data reveals no influence of postcollision interaction which may also distort the Auger line shape in the threshold region. Finally, we note that well above threshold also a pronounced satellite emission is observed $\approx 5 \text{ eV}$ below the 1G_4 line (not shown) which is ascribed to a spectator vacancy transition [20,22]. It is completely absent at resonance.

We now focus on the 1G_4 line and study its evolution when the photon energy is swept through the L_3 excitation

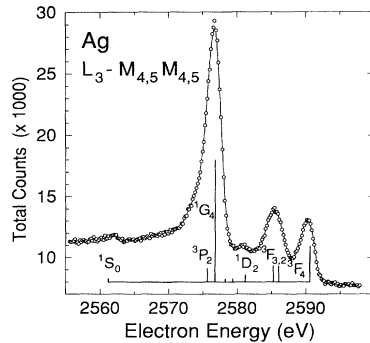


FIG. 1. Resonant Ag $L_3M_{4,5}M_{4,5}$ Auger spectrum excited at 1 eV above the L_3 edge. The theoretical relative multiplet energies and intensities are from [18].

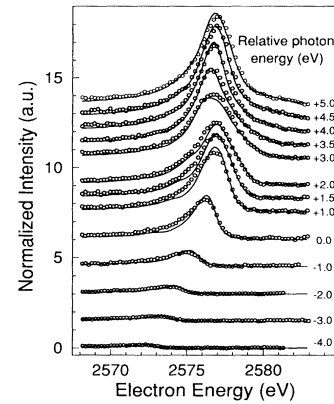


FIG. 2. Dependence of the Ag $L_3M_4M_5(^1G_4)$ line on the exciting photon energy, referenced relative to the Ag L_3 absorption edge. The measured spectra (circles) are normalized to the incoming photon flux and a constant background contribution has been subtracted for each spectrum. The solid lines are the result of the applied numerical model (see text).

threshold (Fig. 2). The spectra are shown as measured, only a constant background contribution has been subtracted. The emission intensity is accurately normalized to the photon flux. Starting at -4 eV relative to threshold, the emission appears to disperse linearly with photon energy and its intensity rapidly increases. Around $+1 \text{ eV}$ the normal Auger transition gradually develops centered around 2576.8 eV . However, the line shape and intensity continues to vary significantly throughout the studied photon energy range above the edge. Examined more closely (Fig. 3), the most dramatic changes occur for subthreshold excitation where an additional structure clearly appears superimposed on the highly asymmetric emission profile.

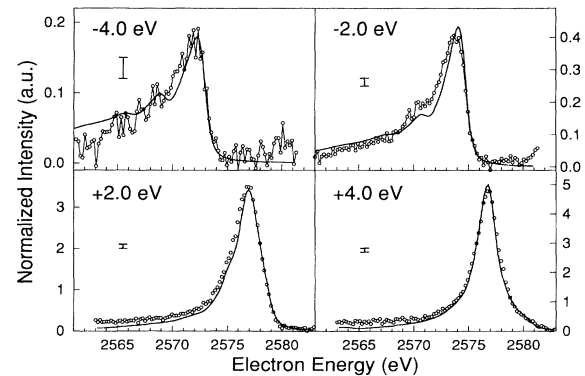


FIG. 3. Subset of the data displayed in Fig. 2. Note the strong variation of the spectral line shape across threshold. The pronounced structure on the low energy side for subthreshold excitation as well as the apparent narrowing at $+4.0 \text{ eV}$ is qualitatively reproduced by the model taking into account the calculated partial density of unoccupied d states.

We argue that this peculiar behavior can be understood as a manifestation of continuouslike radiationless resonant Raman scattering.

To support this argument we have performed a simple

$$i(\epsilon_A, \hbar\omega) = C \int_0^\infty \int_0^\infty \frac{\rho_d(\epsilon) N_{\text{ph}}(\hbar\omega - \hbar\omega') d\epsilon d\hbar\omega'}{[(\hbar\omega' - \epsilon - E_{L_3})^2 + \Gamma_{L_3}^2/4][(\hbar\omega' - \epsilon - \epsilon_A - E_{M_4M_5})^2 + \Gamma_{M_4M_5}^2/4]}.$$

N_{ph} is the photon energy distribution in the experiment. The measured spectrum $I(\epsilon_A, \hbar\omega)$ is obtained by convolution with the spectral function N_{el} of the electron analyzer

$$I(\epsilon_A, \hbar\omega) = \int_0^\infty d\epsilon'_A N_{\text{el}}(\epsilon_A - \epsilon'_A) i(\epsilon'_A, \hbar\omega).$$

Both N_{ph} and N_{el} are well represented by Gaussians with the experimentally determined FWHM values. The Fermi energy is taken as the energy reference, and we have $E_{L_3} = 3351$ eV, the L_3 edge position (see above). For the final state, $E_{M_4M_5}$ is obtained from the measured energy E_A of the 1G_4 line well above threshold since $E_A = E_{L_3} - E_{M_4M_5}$. The lifetime width $\Gamma_{L_3} = 2.05 \pm 0.1$ eV is determined from the L_3 photoelectron line excited at 3900 eV. The final state width $\Gamma_{M_4M_5} = 0.58 \pm 0.07$ eV is obtained from the corresponding single hole lifetime widths, derived from photoemission [21].

All matrix elements are included in the constant scale factor C . To model the intermediate dipole transitions of the photoelectron ϵ we use the calculated partial density of empty d states $\rho_d(\epsilon)$ (Fig. 4) and neglect the contribution of s states.

The result of this simple approach (solid line in Figs. 2 and 3) is in surprising agreement with the measured data. We emphasize that this is not a fit, the only adjustable parameter is the scaling factor C , which is the same for all spectra. The shoulder at ≈ 4 eV below the steep rise of the main peak can be related to a corresponding structure around 4 eV in the calculated density of d states (Fig. 4). This arises because by energy conservation $\epsilon = \hbar\omega - E_{M_4M_5} - \epsilon_A$. Therefore, an inverted $\rho_d(-\epsilon_A)$

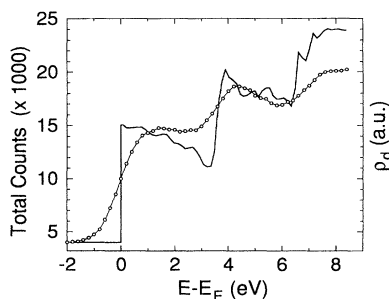


FIG. 4. Calculated partial density ρ_d of unoccupied d states [23] (solid line) in comparison to the measured Ag L_3 near-edge spectrum (open circles) obtained by measuring the intensity of the 1G_4 line as a function of the photon energy. The Fermi energy E_F is identified with the inflection point of the measured edge.

calculation which is based on the results of resonant scattering theory [4]. The energy distribution $i(\epsilon_A)$ of the 1G_4 Auger electrons ϵ_A for the excitation energy $\hbar\omega$ in the threshold region is written as

contributes to the Auger electron distribution, and the Fermi energy $\epsilon = 0$ corresponds to its high energy flank which is rounded off by the final state lifetime and the experimental resolution. This edge also disperses with photon energy below threshold since $\epsilon_A = \hbar\omega - E_{M_4M_5}$.

Above threshold, the normal Auger line develops but the line shape is still strongly modulated by $\rho_d(\epsilon)$. The apparent line narrowing for +4.0 eV excitation is also caused by the same structure in $\rho_d(\epsilon)$. We note that if the final state is kept constant in the experiment, e.g., the 1G_4 emission at its characteristic energy $E_A = E_{L_3} - E_{M_4M_5}$ well above threshold, and its intensity is measured as a function of photon energy, a partial yield absorption spectrum is obtained which is not limited by the intermediate state lifetime [15] (cf. Fig. 4).

All features of the measured threshold spectrum are thus described by this model if the continuous distribution of intermediate states is taken correctly into account via the partial density of empty states. We have shown that it is possible to measure deep inner-shell Auger electron profiles with high accuracy at threshold. Measured structures in these emission profiles can clearly be identified with features in the partial density of states characteristic for the solid state environment. It is worthwhile to finally point out that the observed resonance behavior is universal [4] and also visible similarly in the corresponding radiative process.

We thank Dr. J.E. Müller for providing the results of his density of state calculation.

- [1] See, e.g., *Proceedings of the 2nd International Workshop on Auger Spectroscopy and Electronic Structure*, edited by K. Wandelt, C.-O. Almbladh, and R. Nyholm [Phys. Scr. **T41** (1992)].
- [2] C. O. Almbladh and L. Hedin, in *Handbook on Synchrotron Radiation*, edited by E. E. Koch (North-Holland, Amsterdam, 1983), Vol. 1, Chap. 8, and references therein.
- [3] T. Åberg, Phys. Scr. **T41**, 71 (1992).
- [4] T. Åberg and B. Crasemann, in *Resonant Anomalous X-ray Scattering*, edited by G. Materlik, C.J. Sparks, and K. Fischer (North-Holland, Amsterdam, 1994), p. 430.
- [5] G.S. Brown, M. H. Chen, B. Crasemann, and G. E. Ice, Phys. Rev. Lett. **45**, 1937 (1980).
- [6] G.B. Armen, T. Åberg, J. Levin, B. Crasemann, M.H. Chen, G.E. Ice, and G.S. Brown, Phys. Rev. Lett. **54**, 1142 (1985).

- [7] M.H. Hecht, F.J. Grunthaler, P. Pianetta, H.Y. Cho, M.L. Shek, and P. Mahowald, in *EXAFS and Near Edge Structure III*, edited by K.O. Hodgson, B. Hedman, and J.E. Penner-Hahn (Springer, Berlin, 1984), p. 67.
- [8] A. Kivimäki, H. Aksela, S. Aksela, and O.-P. Sairanen, *Phys. Rev. B* **47**, 4181 (1993).
- [9] M. Elango, A. Ausmees, A. Kikas, E. Nommiste, R. Ruus, A. Saar, J.F. van Acker, J.N. Andersen, R. Nyholm, and I. Martinson, *Phys. Rev. B* **47**, 11 736 (1993).
- [10] A. Kivimäki, A. Naves de Brito, S. Aksela, H. Aksela, O.-P. Sairanen, A. Ausmees, S.J. Osborne, L.B. Dantas, and S. Svensson, *Phys. Rev. Lett.* **71**, 4307 (1993).
- [11] W. Drube, A. Lessmann, and G. Materlik, in *Resonant Anomalous X-ray Scattering*, edited by G. Materlik, C.J. Sparks, and K. Fischer (North-Holland, Amsterdam, 1994), p. 473.
- [12] Z.F. Liu, G.M. Bancroft, K.H. Tan, and M. Schachter, *Phys. Rev. Lett.* **72**, 621 (1994).
- [13] Y. Baba, T.A. Sasaki, and H. Yamamoto, *Phys. Rev. B* **49**, 709 (1994).
- [14] H. Wang, J.C. Woicik, T. Åberg, M.H. Chen, A. Herrera-Gomez, T. Kendelewicz, A. Mäntykenttä, K.E. Miyano, S. Southworth, and B. Crasemann, *Phys. Rev. A* **50**, 1359 (1994).
- [15] W. Drube, A. Lessmann, and G. Materlik, *Jpn. J. Appl. Phys.* **32**, Suppl. 32-2, 173 (1993).
- [16] W. Drube, H. Schulte-Schrepping, H.-G. Schmidt, R. Treusch, and G. Materlik, *Rev. Sci. Instrum.* (to be published).
- [17] J.A. Bearden and A.F. Burr, *Rev. Mod. Phys.* **39**, 125 (1967).
- [18] J.-M. Mariot and M. Ohno, *Phys. Rev. B* **34**, 2182 (1986).
- [19] G.G. Kleiman, S.G.C. de Castro, and R. Landers, *Phys. Rev. B* **49**, 2753 (1994).
- [20] G.G. Kleiman, R. Landers, and S.G.C. de Castro, *J. El. Spec. Rel. Phenomena* **68**, 329 (1994).
- [21] N. Mårtensson and R. Nyholm, *Phys. Rev. B* **24**, 7121 (1981).
- [22] S.L. Sorensen, R. Carr, S.J. Schaphorst, S.B. Whitfield, and B. Crasemann, *Phys. Rev. B* **39**, 6241 (1989).
- [23] J.E. Müller (private communication). The calculation uses the LAPW method, see also J.E. Müller and J.W. Wilkins, *Phys. Rev. B* **29**, 4331 (1984).